Molecular Design and Optimization of ^{99m}Tc-Labeled Recombinant Affibody Molecules Improves Their Biodistribution and Imaging Properties

Helena Wållberg[1], Anna Orlova[2], Mohammed Altai[2], Seyed Jalal Hosseinimehr[2,3], Charles Widström[4], Jennie Malmberg[2], Stefan Ståhl[1], and Vladimir Tolmachev[2]

[1]Division of Molecular Biotechnology, School of Biotechnology, AlbaNova University Center, Royal Institute of Technology, Stockholm, Sweden; [2]Division of Biomedical Radiation Sciences, Department of Radiology, Oncology and Clinical Immunology, Rudbeck Laboratory, Uppsala University, Uppsala, Sweden; [3]Department of Radiopharmacy, Faculty of Pharmacy, Mazandaran University of Medical Sciences, Sari, Iran; and [4]Hospital Physics, Department of Oncology, Uppsala University Hospital, Uppsala, Sweden

Affibody molecules are a recently developed class of targeting proteins based on a nonimmunoglobulin scaffold. The small size (7 kDa) and subnanomolar affinity of Affibody molecules enables high-contrast imaging of tumor-associated molecular targets, particularly human epidermal growth factor receptor type 2 (HER2). ^{99m}Tc as a label offers advantages in clinical practice, and earlier studies demonstrated that ^{99m}Tc-labeled recombinant Affibody molecules with a C-terminal cysteine could be used for HER2 imaging. However, the renal retention of radioactivity exceeded tumor uptake, which might complicate imaging of metastases in the lumbar region. The aim of this study was to develop an agent with low renal uptake and preserved tumor targeting. **Methods:** A series of recombinant derivatives of the HER2-binding $Z_{HER2:342}$ Affibody molecule with a C-terminal chelating sequence, –GXXC (X denoting glycine, serine, lysine, or glutamate), was designed. The constructs were labeled with ^{99m}Tc and evaluated in vitro and in vivo. **Results:** All variants were stably labeled with ^{99m}Tc, with preserved capacity to bind specifically to HER2-expressing cells in vitro and in vivo. The composition of the chelating sequence had a clear influence on the cellular processing and biodistribution properties of the Affibody molecules. The best variant, ^{99m}Tc-$Z_{HER2:V2}$, with the C-terminal chelating sequence –GGGC, provided the lowest radioactivity retention in all normal organs and tissues including the kidneys. ^{99m}Tc-$Z_{HER2:V2}$ displayed high uptake of radioactivity in HER2-expressing xenografts, 22.6 ± 4.0 and 7.7 ± 1.5 percentage injected activity per gram of tissue at 4 h after injection in SKOV-3 (high HER2 expression) and DU-145 (low HER2 expression) tumors, respectively. In both models, the tumor uptake exceeded the renal uptake. **Conclusion:** These results demonstrate that the biodistribution properties of recombinant ^{99m}Tc-labeled Affibody molecules can be optimized by modification of the C-terminal cysteine-containing chelating sequence. ^{99m}Tc-$Z_{HER2:V2}$ is a promising candidate for further development as a diagnostic radiopharmaceutical for imaging of HER2-expressing tumors. These results may be useful for the development of imaging agents based on other Affibody molecules and, hopefully, other scaffolds.

Key Words: Affibody molecule; ^{99m}Tc; molecular imaging; HER2; C-terminal cysteine

Overexpression of human epidermal growth factor receptor type 2 (HER2) provides tumors with a growth advantage and is a part of the malignant phenotype (*1*). The use of HER2-targeting monoclonal antibodies or tyrosine kinase inhibitors increases survival of patients with disseminated HER2-expressing breast cancer (*2,3*). Detection of HER2 expression in vivo is necessary to stratify patients for HER2-targeting therapy (*4–6*). Molecular imaging has the potential to visualize HER2 expression in both primary tumors and metastases in a single noninvasive procedure (*7*). Several types of HER2-targeting imaging agents have been evaluated for this purpose (*7,8*). Affibody molecules (Affibody AB), small (7 kDa) engineered affinity proteins, constitute a promising class of tracers for imaging (*9,10*). Several variants of the $Z_{HER2:342}$ anti-HER2 Affibody molecule have been labeled with various nuclides and enabled high-contrast imaging of HER2-expressing xenografts in mice (*9,10*). Moreover, ^{111}In- and ^{68}Ga-labeled variants of this molecule have been used for clinical imaging of HER2-expressing metastases (*11*).

^{99m}Tc (half-life, 6 h; γ-energy, 140.5 keV) is a commonly used nuclide in molecular imaging applications because of its photon energy (nearly ideal for SPECT), low cost, excellent availability, and low absorbed-dose burden to the patient. Recently, several approaches to label the HER2-binding Affibody molecule $Z_{HER2:342}$ and its derivatives with ^{99m}Tc have been evaluated (*12–21*). Variants and positioning of histidine tags, as well as mercaptoacetyl-

or cysteine-containing peptide-based chelators, were evaluated for the coordination of ^{99m}Tc. Results from the biodistribution studies demonstrated that the derivatives of $Z_{HER2:342}$ were cleared from the body mainly via glomerular filtration, followed by a high degree of renal reabsorption leading to a high level of renal retention of radioactivity when residualizing labels were used. Moreover, the use of hexahistidine tags for labeling and purification was shown to cause an unwanted, elevated hepatic uptake of radioactivity (12,19,22,23). The evaluation of peptide-based chelators positioned at the N-terminus of the tracer revealed that the amino acid composition of the N-terminus was critical for the biodistribution profile in terms of liver uptake and the extent of hepatobiliary excretion. The use of amino acids with hydrophilic (polar or charged) side chains in the N-terminal chelators provided reduced liver uptake and low levels of hepatobiliary excretion (14,16–18,22), whereas the composition of the C-terminus was shown to be less influential in that aspect (23). However, in agreement with previously published data on chelator stability and biodistribution of ^{99m}Tc-labeled proteins (24–26), the use of an N_3S cysteine–based chelator at the C-terminus provided appreciably less release of ^{99m}Tc-pertechnetate in the circulation than did the SN_3 chelator at the N-terminus (15,19,21). Furthermore, Ala^1,Glu^2 at the N-terminus has been shown to be associated with low hepatic uptake and low hepatobiliary excretion (19,21–23). A more detailed summary of previous results and the influence of chelators on the biodistribution of Affibody molecules is provided in the supplemental materials (available online only at http://jnm.snmjournals.org).

On the basis of our observations, we hypothesized that Affibody molecules containing the amino acid sequences AEN$^−$ at the N-terminus and the –GGGC, –GGSC, –GGEC, or –GGKC peptide–based chelators (Fig. 1) at the C-terminus could be labeled with ^{99m}Tc, with preserved binding specificity to HER2; would be stable in the circulation; would be cleared from blood circulation predominantly by renal excretion; and would yield low renal retention of radioactivity.

To verify this hypothesis, 4 $Z_{HER2:342}$ Affibody variants were generated (Fig. 2), labeled with ^{99m}Tc, and evaluated in vitro and in vivo. For comparison, an anti-HER2 Affibody molecule, $Z_{HER2:V1}$, which is homologous to the previously studied PEP05352 (21) (an Affibody molecule
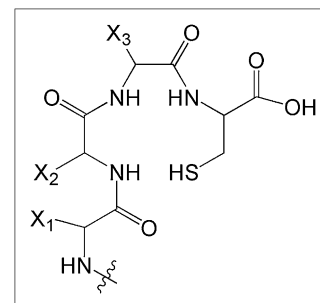
FIGURE 1. General structure of N_3S chelator formed by C-terminal cysteine and adjacent amino acids.

displaying low retention of ^{99m}Tc radioactivity in the kidneys) but that does not contain any scaffold modifications or C-terminal glycine, was included in the study.

MATERIALS AND METHODS

Materials

α-D-gluconic acid sodium salt and ethylenediaminetetraacetic acid were from Sigma-Aldrich, and tin(II)-chloride dehydrate and pyridine were from Fluka Chemika. Phosphate-buffered saline (PBS), pH 7.4, was produced in-house. ^{99m}Tc was obtained as pertechnetate from an Ultra-TechneKow generator (Covidien) eluted with sterile 0.9% sodium chloride (Covidien). An automated γ-counter (Perkin-Elmer) was used to measure the radioactivity. Yield, radiocolloid content, and radiochemical purity of the labeled Affibody constructs were analyzed using 150-771 Dark Green, Tec-Control Chromatography strips from Biodex Medical Systems, as previously described (27). NuPAGE 10% Bis-Tis gels (Invitrogen) were used for analysis of conjugates and in vitro stability studies. The Cyclone Storage Phosphor System and the OptiQuant image analysis software (Perkin-Elmer) were used to measure the radioactivity distribution on chromatography strips and polyacrylamide gel electrophoresis (PAGE) gels.

Preparation of Affibody Molecules

A detailed description of the production, purification, and characterization of the $Z_{HER2:V1}$–$Z_{HER2:V5}$ Affibody molecules is provided elsewhere (28), and some relevant properties are presented in Table 1. All variants are characterized by high melting points (over 63°C) and high affinity (140–260 pM) to HER2. Purified proteins were divided in aliquots of 100 μg and freeze-dried for storage.

Radiolabeling and In Vitro Stability

Radiolabeling was performed using the optimized 2-vial kit method described by Ahlgren et al. (27). For biodistribution studies, conjugates were purified using disposable NAP-5 columns

FIGURE 2. Alignment of studied HER2-binding Affibody molecules. Positions of α-helices 1 through 3 are indicated by boxes. Peptide-based chelators are marked by bold font, and variable amino acids are marked red.

TABLE 1
Properties of Affibody Molecules

Affibody molecule	C-terminus	Molecular weight (Da)	Isoelectric point	Melting point (°C)	On-rate k_a (1/Ms)	Off-rate k_d (1/s)	Dissociation constant K_D (pM)
$Z_{HER2:V1}$	−GSEC	6,758.5	6.42	63	3.29×10^6	4.68×10^{-4}	142
$Z_{HER2:V2}$	−GGGC	6,656.4	8.14	65	4.25×10^6	4.87×10^{-4}	150
$Z_{HER2:V3}$	−GGSC	6,696.5	8.14	66	2.81×10^6	5.29×10^{-4}	188
$Z_{HER2:V4}$	−GGEC	6,728.5	6.42	65	1.94×10^6	4.95×10^{-4}	255
$Z_{HER2:V5}$	−GGKC	6,727.5	8.91	66	4.06×10^6	6.51×10^{-4}	160

(GE Healthcare) preequilibrated with PBS. After purification, the purity was evaluated using instant thin-layer chromatography and cross-validated using radio–sodium dodecyl sulfate (SDS)-PAGE.

For serum stability studies, freshly labeled $Z_{HER2:V1}$-$Z_{HER2:V5}$ (10 μL) was diluted in a serum sample (240 μL) to a concentration similar to the concentration in blood at the moment of injection, incubated for 1 h at 37°C, and analyzed using radio–SDS-PAGE in 2-(N-morpholino)ethanesulfonic acid buffer (200 V constant). A sample of pertechnetate was run in parallel as reference.

In Vitro Cell Studies

The HER2-expressing ovarian cancer cell line SKOV-3, 1.2×10^6 HER2 receptors per cell (29), and the prostate cancer cell line DU-145, 5×10^4 HER2 receptors per cell (Jennie Malmberg, unpublished data, 2010), were used in cell studies. The specificity of radiolabeled Affibody molecules binding to these cells and cellular retention and internalization of radioactivity were evaluated, as described by Wållberg and Orlova (30).

In Vivo Studies

Biodistribution Studies. The animal study was approved by the Local Ethics Committee for Animal Research. In comparative biodistribution studies, non–tumor-bearing NMRI mice were used. The mice were randomly divided into groups of 4. Three groups were intravenously injected with each conjugate (1 μg of Affibody ligand, ~480 kBq in 100 μL of PBS) and euthanized by an intraperitoneal injection of ketamine (Ketalar; Pfizer) and xylazine (Rompun; Bayer) at 1, 4, and 24 h after injection. Blood and organ samples were collected and weighed, and their radioactivity content was measured. The organ uptake values were calculated as percentage injected activity per gram of tissue (%IA/g).

The tumor-targeting properties of the conjugates with the most favorable biodistribution, ^{99m}Tc-$Z_{HER2:V1}$ and ^{99m}Tc-$Z_{HER2:V2}$, were studied in mice bearing SKOV-3 and DU-145 xenografts. For inoculation, 5×10^6 DU-145 cells in Matrigel (BD Biosciences) or 10×10^6 SKOV-3 cells were implanted on the right hind leg of immunodeficient mice. Animals (4 mice per data point)

were injected with 80 kBq of ^{99m}Tc-$Z_{HER2:V1}$ or ^{99m}Tc-$Z_{HER2:V2}$ in 100 μL of PBS. The injected protein dose was 1 μg for mice bearing SKOV-3 tumors and 0.3 μg for DU-145 tumors. Biodistribution and tumor targeting were studied at 4 h after injection. To show specificity of ^{99m}Tc-$Z_{HER2:V2}$ targeting in vivo, 1 group of mice with SKOV-3 and 1 with DU-145 xenografts were preinjected with 1 mg of nonlabeled $Z_{HER2:342}$ at 40 min before the injection of ^{99m}Tc-$Z_{HER2:V2}$. The animals were sacrificed at 4 h after injection, and the radioactivity concentration in blood and tumors was measured.

γ-Camera Imaging. In vivo imaging was performed to obtain a visual confirmation of the biodistribution data. SKOV-3 and DU-145 xenograft–bearing mice were injected with ^{99m}Tc-$Z_{HER2:V1}$ or ^{99m}Tc-$Z_{HER2:V2}$. The mice bearing SKOV-3 xenografts were injected with 0.9 MBq (2 μg), and mice bearing DU-145 xenografts with 0.85 MBq (0.3 μg). Immediately before imaging, at 4 h after injection, the animals were sacrificed, and the urinary bladders were excised. The imaging experiment was performed using a Infinia γ-camera (GE Healthcare) equipped with a low-energy high-resolution collimator. Static images (30 min) were obtained with a zoom factor of 2 in a 256×256 matrix.

RESULTS

Radiolabeling and In Vitro Stability

The results of radiolabeling and stability tests are presented in Table 2. The use of an optimized procedure (27) provided labeling yields over 90% for all conjugates and a radiocolloid content below 3%. Purification using disposable NAP-5 columns provided radiochemical purity over 98%.

Figure 3 shows a representative radioactivity distribution in SDS-PAGE gel after incubation in murine blood plasma at 37°C for 60 min. The main peak corresponded to the monomeric Affibody molecule. No peaks indicating aggregation of Affibody molecules or transchelation of the radio-

TABLE 2
Labeling of Affibody Molecules

Affibody molecule	Labeling yield (%)	Radiochemical purity after size-exclusion chromatography purification (%)	Stability (loss of label after 1 h of incubation in murine serum at 37°C) (%)
$Z_{HER2:V1}$	95.5 ± 1.4	98.2 ± 1.5	2.9 ± 1
$Z_{HER2:V2}$	92.0 ± 3.1	99.9 ± 0.2	3.3 ± 0.1
$Z_{HER2:V3}$	97.2 ± 1.4	99.6 ± 0.3	0
$Z_{HER2:V4}$	96.6 ± 0.9	99.5 ± 0.2	0.05 ± 0.05
$Z_{HER2:V5}$	96.2 ± 0.2	99.4 ± 0.3	0.3 ± 0
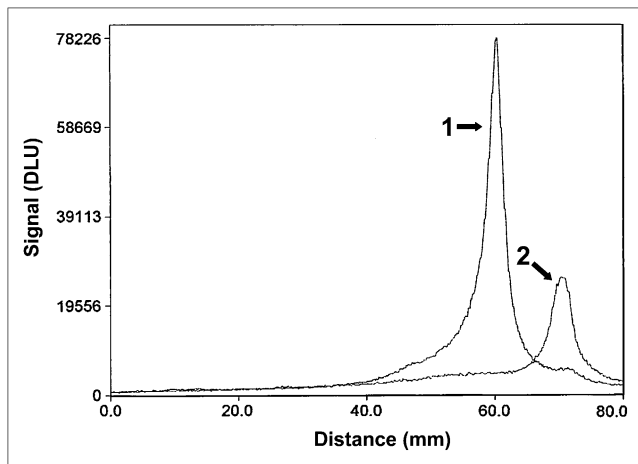
FIGURE 3. Representative SDS-PAGE analysis of stability of ^{99m}Tc-labeled Affibody molecules (^{99m}Tc-Z$_{HER2:V2}$) in serum. 1. ^{99m}Tc-Z$_{HER2:V2}$ incubated in murine serum at 37°C for 1 h; 2. ^{99m}TcO$_4^-$ used as marker for low-molecular-weight compounds. Signal, measured as digital light units, is in proportion to radioactivity in given point of lane in SDS-PAGE gel. DLU = digital light units.

nuclide to blood plasma proteins were observed. The only other observed radioactivity peak corresponded to low-molecular-weight compounds, such as ^{99m}Tc-pertechnetate. This peak did not contain more than 3.5% of the total activity at the end of the stability test (Table 2).

In Vitro Cell Studies

Binding specificity tests (Table 3) indicated that the binding of all ^{99m}Tc-labeled Affibody constructs to HER2-expressing cells was receptor-mediated because saturation of the receptors by preincubation with nonlabeled Z$_{HER2:342}$ significantly decreased the binding of the radiolabeled Affibody molecule.

Cellular Retention and Internalization Experiments. The results of the cellular retention and internalization experiments are presented in Figure 4. A general feature of all conjugates was the low contribution from internalized radioactivity to the overall cell-bound radioactivity. Instead, the main source of the cell-associated radioactivity was from membrane-bound conjugates. Even after 24 h of incubation, the fraction of internalized radioactivity was in the range of 12%–24% for all conjugates. However, an appreciable difference in cellular retention of the conjugates could be seen. The highest retention was achieved with ^{99m}Tc-Z$_{HER2:V5}$, with 75.0% ± 0.5% of the radioactivity still associated with cells after 24 h, followed by ^{99m}Tc-Z$_{HER2:V4}$ (64.6% ± 0.7% at 24 h). ^{99m}Tc-Z$_{HER2:V1}$ and ^{99m}Tc-Z$_{HER2:V3}$ demonstrated an intermediate retention, 53.3% ± 1.0% and 55.8% ± 2.3%, respectively, after 24 h. The retention level of ^{99m}Tc-Z$_{HER2:V2}$ (47.5% ± 0.4% at 24 h) was the lowest. Still, the difference in cellular retention after 4 h (a time point relevant for in vivo imaging), was not substantial, and 80%–88% of the initially bound radioactivity was still cell-associated at that time point for all conjugates.

In Vivo Studies

Biodistribution Studies. Data on the comparative biodistribution of the ^{99m}Tc-labeled Affibody molecules in male NMRI mice at 1, 4, and 24 h after intravenous injection are presented in Supplemental Table 2. The general pattern of all 5 conjugates was typical for Affibody molecules, with a rapid clearance from the blood, nonspecific compartments, and carcass. The average radioactivity in the gastrointestinal tract, including its content, was below 4% for all conjugates, showing minimal excretion of the conjugates or their radiocatabolites via bile. The low levels of radioactivity uptake in the stomach and salivary gland suggested that the release of ^{99m}Tc-pertechnetate in vivo was negligible. There were, however, substantial differences in the biodistribution profiles of Affibody molecules labeled using different N$_3$S chelators. The pulmonary uptake at 4 h after injection was significantly higher for ^{99m}Tc-Z$_{HER2:V4}$ and ^{99m}Tc-Z$_{HER2:V5}$, containing charged amino acids (glutamic acid and lysine, respectively) in the chelating moiety. The hepatic uptake of ^{99m}Tc-Z$_{HER2:V5}$ was 2- to 3-fold higher than the uptake of any of the other conjugates included in the study. Moreover, this conjugate also showed a substantially elevated uptake in the spleen at both 4 and 24 h after injection.

TABLE 3
Specificity of Binding of ^{99m}Tc-Labeled Affibody Molecules to HER2-Expressing Cells In Vitro

| | Cell-associated radioactivity (% of added) | | | |
| | DU-145 | | SKOV-3 | |
Affibody molecule	No presaturation	After presaturation	No presaturation	After presaturation
^{99m}Tc-Z$_{HER2:V1}$	11.4 ± 0.2	1.2 ± 0.3	40.4 ± 0.4	1.0 ± 0.2
^{99m}Tc-Z$_{HER2:V2}$	9.3 ± 0.6	1.48 ± 0.05	42.9 ± 1.4	1.8 ± 0.1
^{99m}Tc-Z$_{HER2:V3}$	10.2 ± 0.9	1.4 ± 0.2	51.2 ± 1.7	1.5 ± 0.1
^{99m}Tc-Z$_{HER2:V4}$	8.8 ± 0.4	2.0 ± 0.3	53.1 ± 4.5	3.9 ± 0.2
^{99m}Tc-Z$_{HER2:V5}$	9.0 ± 0.45	1.6 ± 0.2	53.9 ± 1.3	4.7 ± 0.6

Specificity test was performed using DU-145 prostate cancer and SKOV-3 ovarian cancer cell lines. For presaturation of HER2, a 500-fold molar excess of nonradioactive Affibody molecule was added. Data are presented as mean values from 3 cell dishes with SD. Presaturation of HER2 caused significant decrease of binding, which demonstrated specific binding to HER2.
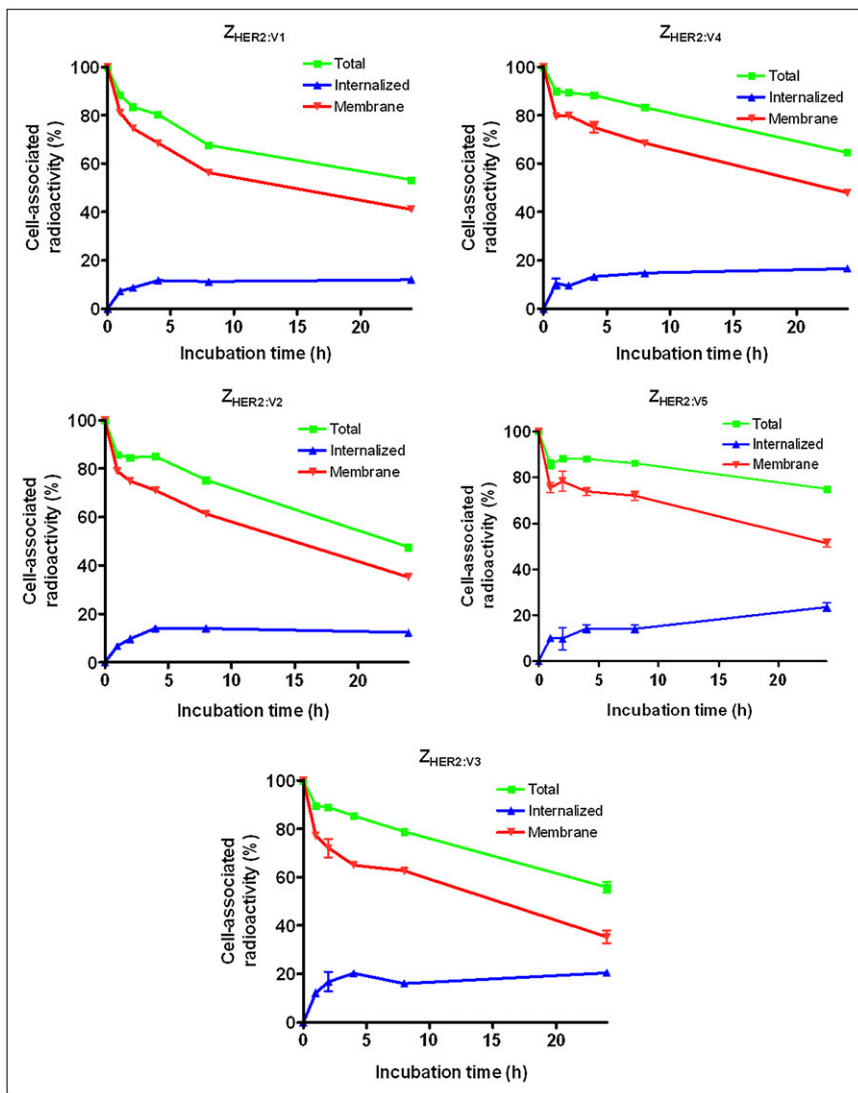
FIGURE 4. Cell-associated radioactivity as function of time after interrupted incubation of SKOV-3 cells with ^{99m}Tc-labeled Affibody molecules. Cell-associated radioactivity at time zero after interrupted incubation was considered 100%. Data are presented as average value from 3 dishes $\pm$ SD. Error bars might not be seen because they are smaller than point symbols.

The most remarkable difference between the conjugates was the large difference in renal retention of radioactivity. Already at 1 h after injection, ^{99m}Tc-$Z_{HER2:V4}$ and ^{99m}Tc-$Z_{HER2:V5}$ demonstrated the highest radioactivity accumulation in the kidneys. ^{99m}Tc-$Z_{HER2:V1}$ and ^{99m}Tc-$Z_{HER2:V3}$ showed intermediate values, and ^{99m}Tc-$Z_{HER2:V2}$ demonstrated remarkably low kidney-associated radioactivity, 24 $\pm$ 6 %IA/g already this shortly after injection. The renal accumulation of radioactivity was the lowest with ^{99m}Tc-$Z_{HER2:V2}$ at all studied time points. The pattern of renal retention of radioactivity after administration of ^{99m}Tc-$Z_{HER2:V4}$ differed from the pattern seen with the other constructs. At 1 h after injection, the radioactivity in the kidneys was as high as the level seen with ^{99m}Tc-$Z_{HER2:V5}$. However, at 4 h after injection the level seen with ^{99m}Tc-$Z_{HER2:V4}$ was only slightly higher than the levels seen with ^{99m}Tc-$Z_{HER2:V1}$ and ^{99m}Tc-$Z_{HER2:V2}$.

The data concerning the biodistribution of ^{99m}Tc-$Z_{HER2:V1}$ and ^{99m}Tc-$Z_{HER2:V2}$ in mice bearing SKOV-3 and DU-145 xenografts are presented in Tables 4 and 5 and Figure 5.

Both conjugates displayed equally good targeting properties in both xenograft models. The presaturation of HER2 receptors with nonlabeled $Z_{HER2:342}$ caused a statistically significant reduction in radioactivity accumulation in both xenograft models, suggesting specificity of the tumor accumulation of ^{99m}Tc-$Z_{HER2:V2}$ (Fig. 5). In agreement with the data obtained from normal mice, the renal uptake was appreciably reduced in the case of ^{99m}Tc-$Z_{HER2:V2}$ in comparison with ^{99m}Tc-$Z_{HER2:V1}$. The reduction was 3-fold for NMRI *nu/nu* mice and 3.4-fold for BALB/C mice. In both models, the administration of ^{99m}Tc-$Z_{HER2:V2}$ resulted in a higher uptake of radioactivity in the tumor than in the kidneys, whereas the situation was reversed for ^{99m}Tc-$Z_{HER2:V1}$. Moreover, with ^{99m}Tc-$Z_{HER2:V2}$, significantly less radioactivity accumulated in several other organs, resulting in an overall increase in tumor-to-organ ratios (Tables 4 and 5).

γ-Camera Imaging. γ-camera imaging, performed at 4 h after injection (Fig. 6), confirmed the results of the biodistribution experiments. Both conjugates were capable of high-contrast imaging of HER2-expressing tumors. How-

TABLE 4

Biodistribution of ^{99m}Tc-$Z_{HER2:V1}$ and ^{99m}Tc-$Z_{HER2:V2}$ Affibody Molecules in Female BALB/c *nu/nu* Mice Bearing SKOV-3 Xenografts at 4 Hours After Intravenous Injection

Organ	Uptake (%IA/g)		Tumor-to-organ ratio	
	^{99m}Tc-$Z_{HER2:V1}$	^{99m}Tc-$Z_{HER2:V2}$	^{99m}Tc-$Z_{HER2:V1}$	^{99m}Tc-$Z_{HER2:V2}$
Blood	0.29 ± 0.03*	0.12 ± 0.01	76 ± 7*	186 ± 29
Lung	0.46 ± 0.10	0.42 ± 0.08	49 ± 9	55 ± 11
Liver	1.4 ± 0.1*	0.93 ± 0.09	15 ± 1*	24 ± 3
Spleen	0.35 ± 0.06	0.42 ± 0.05	64 ± 11	53 ± 6
Stomach	0.4 ± 0.2	0.20 ± 0.07	50 ± 4*	85 ± 7
Kidney	28.0 ± 2.0*	8.2 ± 2.9	0.78 ± 0.06*	2.9 ± 0.5
Salivary gland	0.23 ± 0.05*	0.089 ± 0.005	98 ± 15*	254 ± 45
Tumor	22.0 ± 3.3	22.6 ± 4.0		
Muscle	0.08 ± 0.02	0.06 ± 0.04	296 ± 36	420 ± 152
Bone	0.29 ± 0.03*	0.17 ± 0.04	75 ± 10*	137 ± 15
Intestines†	2.4 ± 0.6	2.6 ± 0.9		
Carcass†	2.9 ± 0.3*	1.6 ± 0.1		

*Significant difference between ^{99m}Tc-$Z_{HER2:V1}$ and ^{99m}Tc-$Z_{HER2:V2}$ Affibody molecules.
†Data for intestines with content and carcass are presented as percentage of injected radioactivity per whole sample.
%IA/g = percentage injected activity per gram of tissue.
Average tumor weight was 0.098 ± 0.04 g. Data are presented as average value from 4 animals ± SD.

ever, the use of ^{99m}Tc-$Z_{HER2:V2}$ provided better contrast than the use of ^{99m}Tc-$Z_{HER2:V1}$.

DISCUSSION

The sensitivity of radionuclide molecular imaging depends on the contrast, which in turn depends on the ratio of radioactivity concentration in tumors and healthy tissues. Thus, to obtain maximal contrast the tumor uptake should be increased or the uptake in normal tissues should be decreased as much as possible. In this study, contrast maximization was achieved by minimization of the accumulation in normal tissues. A major focus was on the excretory organs—that is, the liver and kidneys.

The uptake of a protein-based tracer in the liver can occur by several competing and overlapping mechanisms determined by the interaction with different classes of transporter molecules on the hepatocytes. Depending on the molecular characteristics of the radiocatabolites, a radionuclide may be trapped inside the cells (hepatic uptake) or transported into bile (hepatobiliary excretion). A high level of hepatic uptake reduces the sensitivity of imaging and may hamper the detection of liver metastases, whereas

TABLE 5

Biodistribution of ^{99m}Tc-$Z_{HER2:V1}$ and ^{99m}Tc-$Z_{HER2:V2}$ Affibody Molecules in Male NMRI *nu/nu* Mice Bearing DU-145 Xenografts at 4 Hours After Intravenous Injection

| Organ	Uptake (%IA/g)		Tumor-to-organ ratio	
	^{99m}Tc-$Z_{HER2:V1}$	^{99m}Tc-$Z_{HER2:V2}$	^{99m}Tc-$Z_{HER2:V1}$	^{99m}Tc-$Z_{HER2:V2}$
Blood	0.21 ± 0.02*	0.15 ± 0.02	31 ± 4*	52 ± 6
Lung	0.467 ± 0.122	0.34 ± 0.05	15 ± 4	23 ± 6
Liver	1.0 ± 0.2	0.9 ± 0.1	6.4 ± 0.3*	9 ± 1
Spleen	0.23 ± 0.07	0.21 ± 0.02	30 ± 7	37 ± 7
Stomach	0.21 ± 0.07	0.13 ± 0.02	36 ± 14*	60 ± 4
Kidney	10.7 ± 1.4*	3.5 ± 0.3	0.62 ± 0.04*	2.2 ± 0.4
Salivary gland	0.15 ± 0.02*	0.09 ± 0.01	45 ± 9*	90 ± 21
Tumor	6.6 ± 0.7	7.7 ± 1.5		
Muscle	0.055 ± 0.009	0.041 ± 0.008	123 ± 26	197 ± 59
Bone	0.20 ± 0.04	0.18 ± 0.04	34 ± 5*	42 ± 4
Intestines†	2.2 ± 0.7	2.0 ± 1.5		
Carcass†	2.7 ± 0.4	2.3 ± 0.4		

*Significant difference between ^{99m}Tc-$Z_{HER2:V1}$ and ^{99m}Tc-$Z_{HER2:V2}$ Affibody molecules.
†Data for intestines with content and carcass are presented as percentage of injected radioactivity per whole sample.
%IA/g = percentage injected activity per gram of tissue.
Average tumor weight was 0.95 ± 0.06 g. Data are presented as average value from 4 animals ± SD.
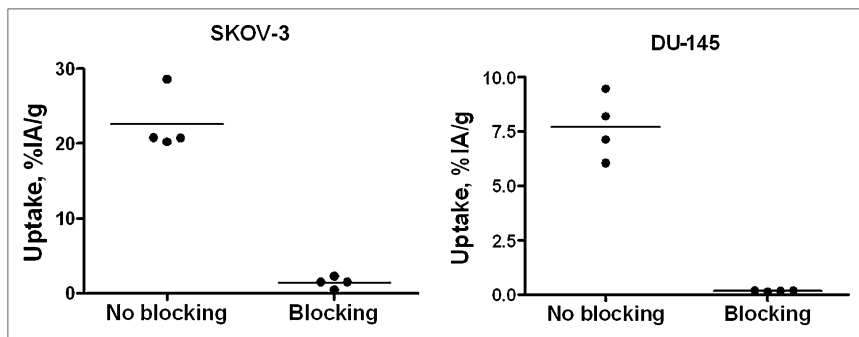
FIGURE 5. In vivo binding specificity of ^{99m}Tc-Z$_{HER2:V2}$ in mice bearing ovarian cancer SKOV-3 and prostate cancer DU-145 xenografts at 4 h after injection. Blocked group was subcutaneously preinjected with excess amount of nonlabeled Z$_{HER2:342}$. Results are presented as percentage of injected activity per gram of tissue (%IA/g).

hepatobiliary excretion creates diffuse background in the abdomen and decreases the sensitivity of detection of extrahepatic abdominal metastases. Because hexahistidine tags cause an elevated hepatic uptake of Affibody molecules (*12,19,22,23*) and their use, thus, should be avoided, a novel antiidiotypic purification strategy has been developed and applied to the constructs used in this study (*28*). Further, N-terminal–placed peptide-based chelators with nonpolar or noncharged side chains were associated with elevated hepatobiliary excretion (*13–16*). This problem seems to have been solved by the placement of peptide-based chelators at the C-terminus and by improving the design of the N-terminus (AEN-) of the Z$_{HER2:VX}$ constructs, adopted from earlier studies (*19,22,31*).

An elevated renal uptake is less critical than hepatobiliary excretion but might complicate the detection of metastases in the lumbar area. The use of nonresidualizing radiohalogen labels for labeling of Affibody molecules provides low renal retention due to efficient washout of the lipophilic radiocatabolites (*32–35*), whereas the use of residualizing radiometal labels leads to high renal retention of radionuclides (*22,31,36*). Because the internalization of Z$_{HER2:342}$ and its derivatives by cancer cells is slow (*19,22,30,31*), residualizing labels are not critical for high tumor uptake shortly after injection, but the tumor uptake is rather determined by the high affinity to HER2. In the kidneys, reabsorption is associated with rapid internalization (*37*), and the use of nonresidualizing labels would provide the advantage of low renal retention of radioactivity. An optimal chelator should provide stable attachment of ^{99m}Tc in the circulation but rapid excretion of radiocatabolites from the kidneys. The design of the Z$_{HER2:VX}$ constructs was based on our previous observation that N$_3$S chelators for the coordination of ^{99m}Tc may provide both residualizing and nonresidualizing properties depending on the amino acids adjacent to the thiol-bearing moiety.

The use of amino acids with electron-donating side chains (serine, lysine, glutamate) close to the mercaptoacetyl in the peptide-based chelators at the N-terminus was associated with stabilization of the ^{99m}Tc chelate in Affibody molecules (*14,16,18*), yielding lower release of ^{99m}Tc-pertechnetate in the circulation. This stabilization effect has also been reported for homologous thiol-containing che-

lators by other researchers (*38*). However, the use of chelators containing several stabilizing side chains caused an elevated renal retention of ^{99m}Tc (*14,16–18*). At the same time, we have found that the renal retention of ^{99m}Tc depends on the relative position of the side chains in the chelators (*17*). It was possible to identify chelators, for example, maESE- (*17*) and maSKS- (*18*), which provided a minimal release of free ^{99m}Tc-pertechnetate in the circulation but caused low radioactivity retention in kidneys due to the rapid excretion of renal low-molecular-weight radiocatabolites (*17*). Unfortunately, the exact mechanism for this phenomenon is unclear, and we pursued the minimization of renal uptake by designing a series of Affibody molecules with homologous chelators for the study of this structure–property relation. Cysteine-containing chelators placed at the C-terminus are intrinsically more stable than cysteine placed at the N-terminus because of a more favorable chelating geometry (*26*). We reasoned that by placing the chelator at the C-terminus, a minimal or no stabilizing effect from electron-donating side chains in the chelating sequence would be required for stability of the ^{99m}Tc-complex in the circulation. Furthermore, the use of polar or charged side chains would not be required to suppress the hepatic uptake when placing the chelators at the C-terminus. At the same time, using a minimal number of stabilizing side chains,
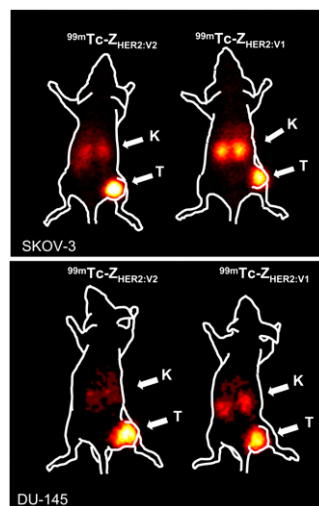
FIGURE 6. Imaging of HER2 expression in SKOV-3 ovarian cancer xenografts (high HER2 expression) in BALB/c *nu/nu* mice and in DU-145 prostate cancer xenografts (moderate HER2 expression) in NMRI *nu/nu* mice using ^{99m}Tc-Z$_{HER2:V1}$ and ^{99m}Tc-Z$_{HER2:V2}$. Planar γ-camera images were acquired at 4 h after injection. Arrows point to tumors (T) and kidneys (K).

the renal retention would be reduced, making the ^{99m}Tc label nonresidualizing.

We have designed 5 novel Affibody constructs with a –GGXC (X denoting glycine, serine, glutamate, or lysine) and –GSEC (homologous to C-terminus of the previous best PEP05352) C-terminal sequence, which could be used for the chelation of ^{99m}Tc. In this way, an amino acid–based chelator was engineered into the Affibody molecules, and no additional processing was required for chelator coupling. The modifications at the C-terminal end insignificantly influenced the affinity of the Affibody molecules to HER2. The radiolabeled Affibody molecules were stable both in vitro (in murine serum) and in vivo. The rapid blood clearance suggests that there was no transchelation to blood proteins from any of the conjugates. Low levels of radioactivity in the stomach and salivary gland indicated that no ^{99m}Tc-pertechnetate was released. The in vitro retention and processing experiments demonstrated an apparent influence of the N$_3$S chelators on the cellular retention of the ^{99m}Tc-Z$_{HER2:V4}$ and ^{99m}Tc-Z$_{HER2:V5}$ conjugates, with the –GGEC and –GGKC chelators providing the strongest cellular retention. The cellular retention of ^{99m}Tc-Z$_{HER2:V2}$ was the lowest, suggesting that the −GGGC chelator provides low residualizing properties to ^{99m}Tc. However, the slow internalization by HER2-expressing cells, which is typical for Z$_{HER2:342}$ derivatives (*19,22,30,31*), leveled out the effect of the chelators. After 4 h of processing (corresponding to an optimal time for imaging), the difference in cellular retention of radioactivity between the 5 conjugates was negligible.

In vivo experiments demonstrated a clear influence from the chelators on the biodistribution of the ^{99m}Tc-labeled Affibody molecules. The positioning of a lysine next to cysteine in Z$_{HER2:V5}$ caused an elevated liver uptake, elevated renal retention, and a slower whole-body clearance. In ^{99m}Tc-maKKK-Z$_{HER2:342}$, the presence of a lysine next to mercaptoacetyl had a similar effect (*18*). Although the molecular mechanism of this effect is unclear, lysine should probably be avoided in this position. The other conjugates displayed a similar distribution of radioactivity in most of the organs except for the kidneys. The effect of the chelator on kidney retention was striking; at 4 h after injection, the difference in renal accumulations was 19-fold (Supplemental Table 2). At all time points, the lowest level of radioactivity in the kidneys was observed with ^{99m}Tc-Z$_{HER2:V2}$.

^{99m}Tc-Z$_{HER2:V2}$ provided one of the lowest levels of renal radioactivity among all previously evaluated ^{99m}Tc-labeled Affibody molecules (*12–21*). It is likely that the low retention of ^{99m}Tc-Z$_{HER2:V2}$–associated radioactivity in kidneys was due to the absence of stabilizing effects from adjacent electron-donating side chains. The renal uptake of ^{99m}Tc-Z$_{HER2:V2}$ was as low as what was obtained with ^{99m}Tc-maGGG-Z$_{HER2:342}$ (*13*), but ^{99m}Tc-Z$_{HER2:V2}$ provided a much lower level of hepatobiliary excretion. The advantage of the −GGGC chelator is clearly seen in comparison with ^{99m}Tc-CGGG-Z$_{HER2:342}$ (*15*). Evidently,

^{99m}Tc-Z$_{HER2:V2}$ is more stable in the circulation than its mirror counterpart—this higher stability manifested as lower levels of radioactivity in the stomach and salivary gland. In addition, ^{99m}Tc-Z$_{HER2:V2}$ displayed lower levels of hepatobiliary excretion due to the optimal design of the N-terminus. Furthermore, excellent biodistribution and targeting properties of ^{99m}Tc-Z$_{HER2:V2}$ was demonstrated in mice bearing HER2-expressing xenografts.

CONCLUSION

The use of a –GGGC N$_3$S chelator at the C-terminal end of anti-HER2 Z$_{HER2:342}$ Affibody molecules enables stable labeling with technetium, with preserved binding specificity. The substitution of a single amino acid in the chelating sequence can modify the targeting properties of radiolabeled conjugates and the cellular processing and retention of radioactivity by cancer cells. In vivo, modification of the amino acid composition of the chelating moiety can cause a substantial difference in the accumulation of radioactivity in excretory organs, emphasizing the importance of careful optimization of the labeling chemistry in the development of targeting proteins. This information might, hopefully, be useful for other researchers working with scaffold-based targeting proteins.

REFERENCES

1. Burstein HJ. The distinctive nature of HER2-positive breast cancers. *N Engl J Med.* 2005;353:1652–1654.
2. Collins D, Hill AD, Young L. Lapatinib: a competitor or companion to trastuzumab? *Cancer Treat Rev.* 2009;35:574–581.
3. Brufsky A. Trastuzumab-based therapy for patients with HER2-positive breast cancer: from early scientific development to foundation of care. *Am J Clin Oncol.* 2010;33:186–195.
4. Esteva FJ, Yu D, Hung MC, Hortobagyi GN. Molecular predictors of response to trastuzumab and lapatinib in breast cancer. *Nat Rev Clin Oncol.* 2010;7:98–107.
5. Frederick PJ, Straughn JM Jr, Alvarez RD, Buchsbaum DJ. Preclinical studies and clinical utilization of monoclonal antibodies in epithelial ovarian cancer. *Gynecol Oncol.* 2009;113:384–390.
6. Ziada A, Barqawi A, Glode LM, et al. The use of trastuzumab in the treatment of hormone refractory prostate cancer; phase II trial. *Prostate.* 2004;60:332–337.
7. Tolmachev V. Imaging of HER-2 overexpression in tumors for guiding therapy. *Curr Pharm Des.* 2008;14:2999–3011.
8. Dijkers EC, de Vries EG, Kosterink JG, Brouwers AH, Lub-de Hooge MN. Immunoscintigraphy as potential tool in the clinical evaluation of HER2/neu targeted therapy. *Curr Pharm Des.* 2008;14:3348–3362.
9. Ahlgren S, Tolmachev V. Radionuclide molecular imaging using Affibody molecules. *Curr Pharm Biotechnol.* 2010;11:581–589.
10. Löfblom J, Feldwisch J, Tolmachev V, Carlsson J, Ståhl S, Frejd FY. Affibody molecules: engineered proteins for therapeutic, diagnostic and biotechnological applications. *FEBS Lett.* 2010;584:2670–2680.
11. Baum RP, Prasad V, Müller D, et al. Molecular imaging of HER2-expressing malignant tumors in breast cancer patients using synthetic ^{111}In- or ^{68}Ga-labeled Affibody. *J Nucl Med.* 2010;51:892–897.
12. Orlova A, Nilsson F, Wikman M, Ståhl S, Carlsson J, Tolmachev V. Comparative in vivo evaluation of iodine and technetium labels on anti-HER2 Affibody for single-photon imaging of HER2 expression in tumors. *J Nucl Med.* 2006;47:512–519.

13. Engfeldt T, Orlova A, Tran T, et al. Imaging of HER2-expressing tumours using a synthetic Affibody molecule containing the 99mTc-chelating mercaptoacetyl-glycyl-glycyl-glycyl (MAG3) sequence. *Eur J Nucl Med Mol Imaging.* 2007;34:722–733.

14. Engfeldt T, Tran T, Orlova A, Widström Ch. Eriksson Karlström A, Tolmachev V. 99mTc-chelator engineering to improve tumour targeting properties of a HER2-specific Affibody molecule. *Eur J Nucl Med Mol Imaging.* 2007;34:1843–1853.

15. Tran T, Engfeldt T, Orlova A, et al. In vivo evaluation of cysteine-based chelators for attachment of 99mTc to tumor-targeting Affibody molecules. *Bioconjug Chem.* 2007;18:549–558.

16. Tran T, Engfeldt T, Orlova A, et al. 99mTc-maEEE-ZHER2:342, an Affibody molecule-based tracer for detection of HER2-expression in malignant tumors. *Bioconjug Chem.* 2007;18:1956–1964.

17. Ekblad T, Tran T, Orlova A, et al. Development and preclinical characterisation of 99mTc-labelled Affibody molecules with reduced renal uptake. *Eur J Nucl Med Mol Imaging.* 2008;35:2245–2255.

18. Tran T, Ekblad T, Orlova A, et al. Effects of lysine-containing mercaptoacetyl-based chelators on the biodistribution of 99mTc-labeled anti-HER2. *Bioconjug Chem.* 2008;19:2568–2576.

19. Ahlgren S, Wållberg H, Tran TA, et al. Targeting of HER2-expressing tumors using a site-specifically 99mTc-labeled recombinant Affibody molecule ZHER2:2395 with C-terminal engineered cysteine. *J Nucl Med.* 2009;50:781–789.

20. Ekblad T, Orlova A, Feldwisch J, Wennborg A, Eriksson Karlström A, Tolmachev V. Positioning of 99mTc-chelators influences radiolabeling, stability and biodistribution of Affibody molecules. *Bioorg Med Chem Lett.* 2009;19:3912–3914.

21. Tran TA, Rosik D, Abrahmsén L, et al. Design, synthesis and biological evaluation of a HER2-specific affibody molecule for molecular imaging. *Eur J Nucl Med Mol Imaging.* 2009;36:1864–1873.

22. Tolmachev V, Hofström C, Malmberg J, et al. HEHEHE-tagged Affibody molecules may be purified by IMAC, are conveniently labeled with [99mTc(CO)3]+, and show improved biodistribution. *Bioconjug Chem.* 2010;21:2013–2022.

23. Ahlgren S, Orlova A, Rosik D, et al. Evaluation of maleimide derivative of DOTA for site-specific labeling of recombinant Affibody molecules. *Bioconjug Chem.* 2008;19:235–243.

24. George AJ, Jamar F, Tai MS, et al. Radiometal labeling of recombinant proteins by a genetically engineered minimal chelation site: technetium-99m coordination by single-chain Fv antibody fusion proteins through a C-terminal cysteinyl peptide. *Proc Natl Acad Sci USA.* 1995;92:8358–8362.

25. Francesconi LC, Zheng Y, Bartis J, Blumenstein M, Costello C, De Rosch MA. Preparation and characterization of [99TcO] apcitide: a technetium labeled peptide. *Inorg Chem.* 2004;43:2867–2875.

26. Davison A, Jones AG, Orvig C, Sohn M. A new class of oxotechnetium(5+) chelate complexes containing a TcON2S2 core. *Inorg Chem.* 1981;20:1629–1632.

27. Ahlgren S, Andersson K, Tolmachev V. Kit formulation for 99mTc-labeling of recombinant anti-HER2 Affibody molecules with a C-terminally engineered cysteine. *Nucl Med Biol.* 2010;37:539–549.

28. Wållberg H, Löfdal PÅ, Tschapalda K. Affinity recovery of eight HER2-binding affibody variants using an anti-idiotypic affibody molecule as capture ligand. *Protein Expr Purif.* 2011;76:127–135.

29. Persson M, Tolmachev V, Andersson K, Gedda L, Sandström M, Carlsson J. [177Lu]pertuzumab: experimental studies on targeting of HER-2 positive tumour cells. *Eur J Nucl Med Mol Imaging.* 2005;32:1457–1462.

30. Wållberg H, Orlova A. Slow internalization of anti-HER2 synthetic affibody monomer 111In-DOTA-ZHER2:342-pep2: implications for development of labeled tracers. *Cancer Biother Radiopharm.* 2008;23:435–442.

31. Ahlgren S, Orlova A, Wållberg H, et al. Targeting of HER2-expressing tumors using 111In-ABY-025, a second generation Affibody molecule with a fundamentally re-engineered scaffold. *J Nucl Med.* 2010;51:1131–1138.

32. Orlova A, Magnusson M, Eriksson T, et al. Tumor imaging using a picomolar affinity HER2 binding Affibody molecule. *Cancer Res.* 2006;66:4339–4348.

33. Kramer-Marek G, Kiesewetter DO, Martiniova L, Jagoda E, Lee SB, Capala J. [18F]FBEM-Z(HER2:342)-Affibody molecule-a new molecular tracer for in vivo monitoring of HER2 expression by positron emission tomography. *Eur J Nucl Med Mol Imaging.* 2008;35:1008–1018.

34. Cheng Z, De Jesus OP, Namavari M, et al. Small-animal PET imaging of human epidermal growth factor receptor type 2 expression with site-specific 18F-labeled protein scaffold molecules. *J Nucl Med.* 2008;49:804–813.

35. Tolmachev V, Mume E, Sjöberg S, Frejd FY, Orlova A. Influence of valency and labelling chemistry on in vivo targeting using radioiodinated HER2-binding. *Eur J Nucl Med Mol Imaging.* 2009;36:692–701.

36. Orlova A, Rosik D, Lundqvist H, Einarsson L, Sandström M, Tolmachev V. Evaluation of 111/114mIn-CHX-A''-DTPA-ZHER2:342, an Affibody ligand conjugate for targeting of HER2-expressing malignant tumours. *Q J Nucl Med Mol Imaging.* 2007;51:314–322.

37. Behr TM, Goldenberg DM, Becker W. Reducing the renal uptake of radiolabeled antibody fragments and peptides for diagnosis and therapy: present status, future prospects and limitations. *Eur J Nucl Med.* 1998;25:201–212.

38. Cyr JE, Koppitz M, Srinivasan A, Dinkelborg LM. Improved peptide chelators for Tc/Re(V); stabilizing side chains [abstract]. *J Labelled Comp Radiopharm.* 2007;50(suppl 1):S9.